Febrile temperatures unmask biophysical defects in $Na_v1.1$ epilepsy mutations supportive of seizure initiation

Linda Volkers,[1,2] Kristopher M. Kahlig,[3] Joost H.G. Das,[1] Marjan J.A. van Kempen,[1] Dick Lindhout,[1] Bobby P.C. Koeleman,[1] and Martin B. Rook[2]

[1]Department of Medical Genetics, Division of Biomedical Genetics, and [2]Department of Medical Physiology, Division of Heart and Lungs, University Medical Center Utrecht, 3508 AB Utrecht, Netherlands
[3]Department of Medicine, Vanderbilt University, Nashville, TN 37235

Generalized epilepsy with febrile seizures plus (GEFS+) is an early onset febrile epileptic syndrome with therapeutic responsive (a)febrile seizures continuing later in life. Dravet syndrome (DS) or severe myoclonic epilepsy of infancy has a complex phenotype including febrile generalized or hemiclonic convulsions before the age of 1, followed by intractable myoclonic, complex partial, or absence seizures. Both diseases can result from mutations in the $Na_v1.1$ sodium channel, and initially, seizures are typically triggered by fever. We previously characterized two $Na_v1.1$ mutants—R859H (GEFS+) and R865G (DS)—at room temperature and reported a mixture of biophysical gating defects that could not easily predict the phenotype presentation as either GEFS+ or DS. In this study, we extend the characterization of $Na_v1.1$ wild-type, R859H, and R865G channels to physiological (37°C) and febrile (40°C) temperatures. At physiological temperature, a variety of biophysical defects were detected in both mutants, including a hyperpolarized shift in the voltage dependence of activation and a delayed recovery from fast and slow inactivation. Interestingly, at 40°C we also detected additional gating defects for both R859H and R865G mutants. The GEFS+ mutant R859H showed a loss of function in the voltage dependence of inactivation and an increased channel use-dependency at 40°C with no reduction in peak current density. The DS mutant R865G exhibited reduced peak sodium currents, enhanced entry into slow inactivation, and increased use-dependency at 40°C. Our results suggest that fever-induced temperatures exacerbate the gating defects of R859H or R865G mutants and may predispose mutation carriers to febrile seizures.

The Journal of General Physiology

INTRODUCTION

Generalized epilepsy with febrile seizures plus (GEFS+) is an autosomal dominant disorder in which subjects have febrile seizures early in childhood, with increased risk for febrile and afebrile seizures later on in life. Fortunately, most patients have spontaneously remitting epilepsy and a normal development (Deprez et al., 2009). Dravet syndrome (DS) is an intractable epilepsy type with poor prognosis, characterized by fever-induced generalized tonic–clonic seizures during the first year of life. Phenotypic progression for DS patients includes complex seizure phenotypes with impairment of psychomotor development, including ataxia and mental disabilities (Deprez et al., 2009). Even though the outcome of these two different epilepsy syndromes differs dramatically, both are associated with the neuronal $Na_v1.1$ ion channel gene *SCN1A* (Escayg et al., 2000; Claes et al., 2003, 2009; Lossin, 2009).

GEFS+ patients harbor predominantly missense mutations, whereas in DS patients, missense, truncation, frameshift, or deletion/duplication mutations have been reported that arise de novo. To date, more than 600 *SCN1A* mutations are associated with a spectrum of epileptic phenotypes, and a few of these missense mutations have been functionally characterized at room temperature to gain insight into the pathophysiology of GEFS+ and DS (Spampanato et al., 2001, 2003, 2004; Lossin et al., 2002, 2003; Rhodes et al., 2004, 2005; Ohmori et al., 2006). When investigated at room temperature, GEFS+ mutant channels exhibit gain-of-function or loss-of-function gating defects, whereas complete loss of ion channel function is common in DS patients (Yu et al., 2006; Ogiwara et al., 2007; Catterall et al., 2010).

Fever-induced seizures are common in GEFS+ and DS subjects and mouse models (Oakley et al., 2009; Martin et al., 2010) and are typically the first reported symptom. However, no study has investigated the role of elevated temperature in the development of gating defects in these mutant channels. Previous functional studies on several other mutated ion channels associated with temperature-induced disorders have already shown that

B.P.C. Koeleman and M.B. Rook contributed equally to this paper.
Correspondence to Linda Volkers: linda.volkers@univ-amu.fr
L. Volkers's present address is Ion Channels and Sensory Transduction Group, Center for Research in Neurobiology and Neurophysiology of Marseille, 13344 Marseille, France.

Abbreviations used in this paper: DS, Dravet syndrome; GEFS+, generalized epilepsy with febrile seizures plus; TTX, tetrodotoxin.

The Rockefeller University Press $30.00
J. Gen. Physiol. Vol. 142 No. 6 641–653
www.jgp.org/cgi/doi/10.1085/jgp.201311042

gating of these ion channels changes at elevated temperatures (Dumaine et al., 1999; Han et al., 2007; Amin et al., 2008; Carle et al., 2009; Samani et al., 2009). We have previously characterized GEFS+ (R859H) and DS (R865G) *SCN1A* mutant channels at room temperature. The R859H mutant showed mixed biophysical gating defects; the R865G mutant showed overall gain-of-function gating defects that could not explain the disease severity of the DS subject (Volkers et al., 2011). Because GEFS+ and DS share fever-associated seizures, we sought to investigate the temperature-dependent gating of the $Na_v1.1$ WT, R859H, and R865G sodium ion channels. We hypothesized that the R859H (GEFS+) and R865G (DS) mutations differentially affect the sodium channel function in a temperature-dependent manner. To test this hypothesis, we characterized the biophysical properties of WT and mutant ion channels at 37 and 40°C.

MATERIALS AND METHODS

Cell culture and transfection

Human-derived tsA201 cells were cultured in Dulbecco's modified Eagle's medium supplemented with 10% FBS, 100 U/ml penicillin, 100 µg/ml streptomycin, and 0.05% L-glutamine in a humidified incubator at 37°C with 5% CO_2. All culture media and supplements were obtained from BioWhittaker. Transient transfections were performed with Lipofectamine (Invitrogen) using in total 6 µg of $Na_v1.1$, β1, and β2 pDNAs in a ratio of 10:1:1, as described previously by Lossin et al. (2002). Cells that expressed β1 and β2 subunits were identified with CD8-positive beads (Invitrogen) and GFP epifluorescence, respectively. Cells that expressed both β subunits were patched 48–72 h after transfection. For electrophysiological measurements, at least two different clones of either WT or mutant constructs were tested. The introduction of R859H (c.G2576A) and R865G (c.G2593G) mutations in the *SCN1A* plasmid DNA (provided by A.L. George Jr., Vanderbilt University, Nashville, TN) has been described previously (Volkers et al., 2011).

Electrophysiological measurements

Before patching, cells were incubated for at least 1 h in cell culture medium containing 140 mM NMDG, 4 mM KCl, 1 mM $CaCl_2$, 1 mM $MgCl_2$, 14.3 mM Na_2HCO_3, 15.1 mM HEPES, 17.5 mM glucose, 1× amino acids (GIBCO), 1× nonessential amino acids (GIBCO), pH 7.35, supplemented with 10% FCS, 100 U/ml penicillin, 100 µg/ml streptomycin, and 2 mM L-glutamine (all from BioWhittaker) in a humidified atmosphere at 37°C, 5% CO_2. For patch experiments, cells were bathed in modified Tyrode's solution containing (mM): 140 NaCl, 5.4 KCl, 1.8 $CaCl_2$, 1 $MgCl_2$, 6 glucose, and 6 HEPES, pH 7.4. $Na_v1.1$ sodium currents were measured at 37 and 40°C using the whole-cell patch-clamp configuration with an amplifier (Axopatch 200B; Molecular Devices). In most cells, electrophysiological parameters were measured at both 37 and 40°C. Patch pipettes were pulled from borosilicate glass capillaries with a pipette puller (P2000; Sutter Instrument) and fire-polished. Patch pipettes had a tip resistance between 1.3 and 2.2 MΩ when filled with the following internal solution (mM): 10 NaF, 110 CsF, 20 CsCl, 2 EGTA, and 10 HEPES, pH 7.35. Cells were allowed to stabilize at room temperature (20–22°C) for 10 min after whole-cell configuration was established. Next, temperature was raised to 37 or 40°C using a temperature-controlled perfusion chamber (Cell MicroControls), and cells were allowed to stabilize at each temperature for ∼7 min. Cells

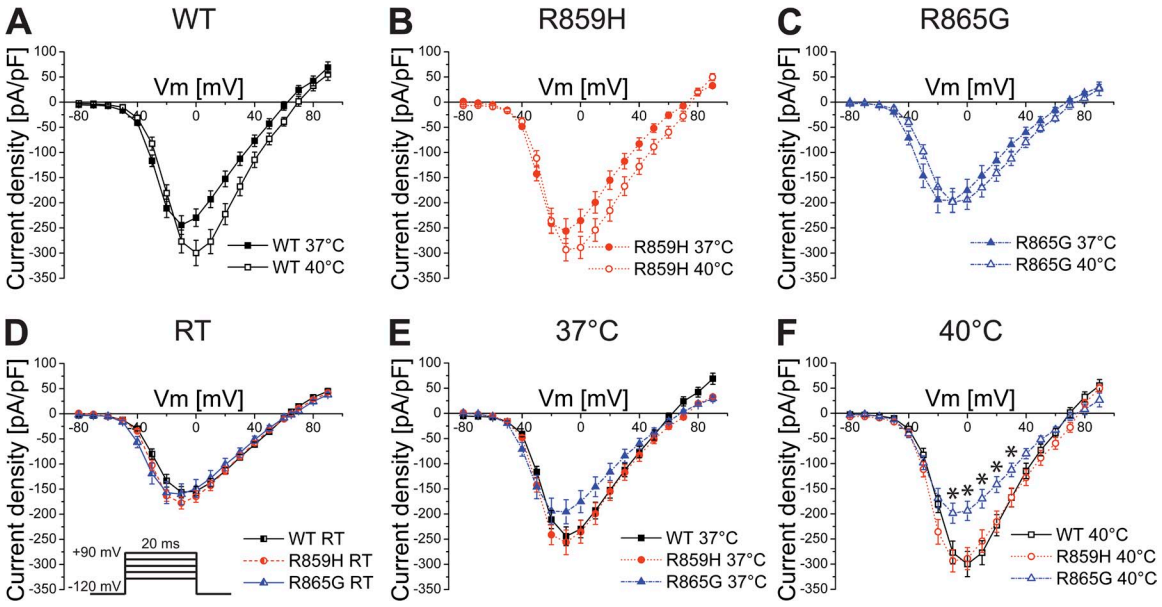

Figure 1. I-V relationships and current densities of $Na_v1.1$ WT (■, 37°C, $n = 13$; □, 40°C, $n = 13$), R859H (●, 37°C, $n = 12$; ○, 40°C, $n = 12$), and R865G (▲, 37°C, $n = 10$; △, 40°C, $n = 10$) ion channels coexpressed with β1 and β2 subunits in tsA201 cells. (A–C) Average I-V relationship for (A) $Na_v1.1$ WT, (B) R859H, and (C) R865G sodium currents consecutively measured at 37 and 40°C, demonstrating decreased R865G current density at physiological and febrile temperatures. Current density was obtained by normalizing peak sodium currents to cell capacitance. (D–F) Average I-V curves of WT, R859H, and R865G measured at (D) room temperature (RT), (E) 37°C, and (F) 40°C, showing a decrease in current density for the DS mutant R865G at 37 and 40°C (*, $P < 0.05$). D, with subtle modification of the y axis and figure symbols and lines, is reprinted with permission from *European Journal of Neuroscience* (Volkers et al., 2011).

expressing sodium current less than −600 pA at room temperature were excluded because of small endogenous sodium currents possibly interfering with the electrophysiological measurements. Cells exhibiting currents greater than −6,000 pA were excluded to avoid voltage-clamp errors. Recordings were ≥90% compensated for pipette series resistance and capacitive transients. Leak currents were subtracted using a $P/4$ procedure. Sodium currents were filtered at 10 kHz and digitized at 100 kHz using a Digidata1322A (Molecular Devices). For analysis, a 5-kHz low pass–filtering step was used. Voltage-clamp protocols were generated and data acquisition was performed using pCLAMP9.2 (Molecular Devices). Voltage-clamp protocols are depicted in the figures where applicable. Steady-state activation was analyzed from consecutive measurements at 37 and 40°C. Current densities were determined by normalizing peak current amplitudes to cell capacitance. Voltage dependence of activation and slow inactivation were determined by fitting the data with a single Boltzmann equation, $I = I_{max}/(1 + \exp((V - V1/2)/k))$, and the

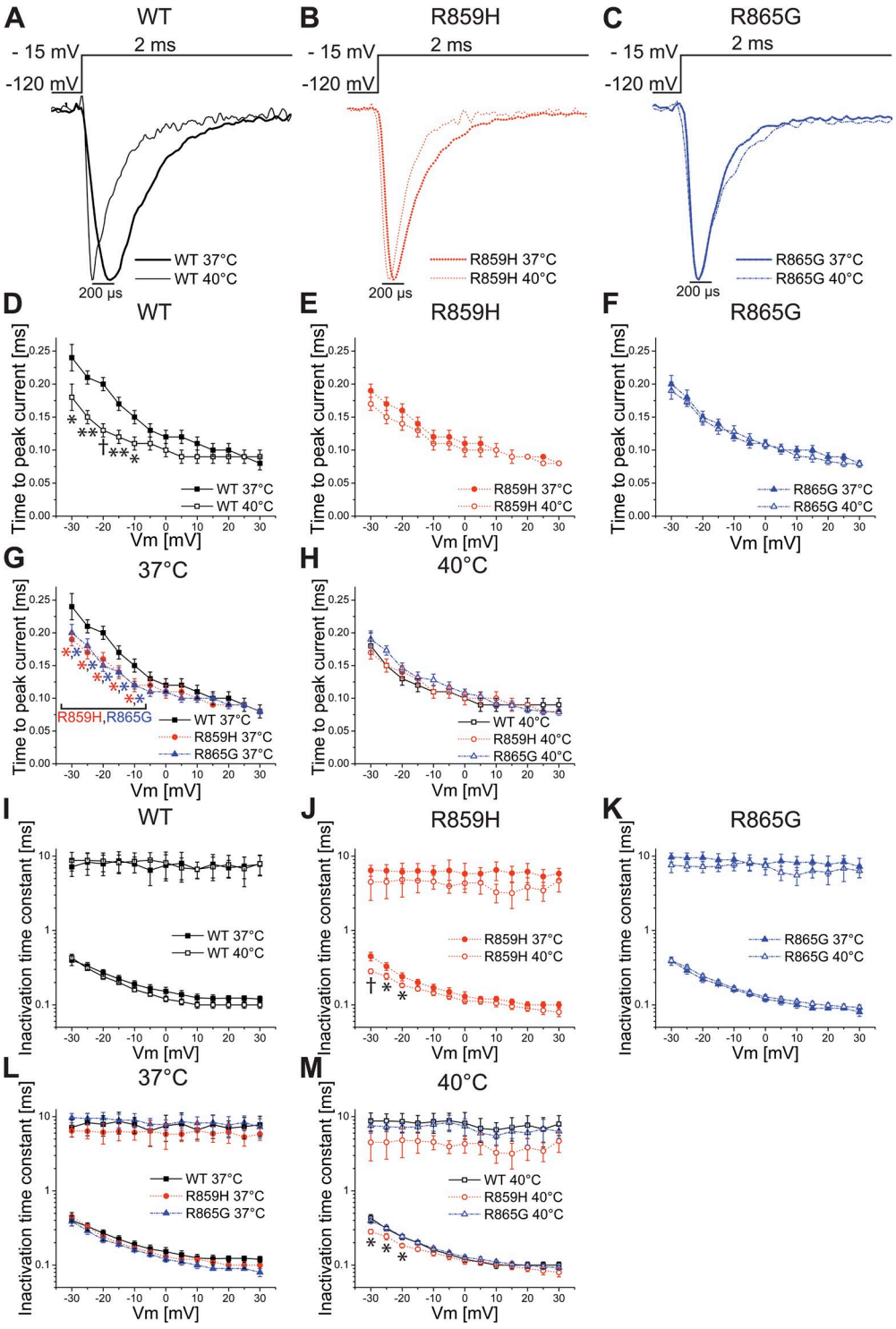

Figure 2. Normalized whole-cell recordings at 37 and 40°C of (A) $Na_v1.1$ WT, (B) R859H, and (C) R865G currents evoked by a depolarizing test pulse to −15 mV from a holding potential of −120 mV. For comparison, recorded currents were normalized to the peak currents. (D–F) Speed of activation was assessed by measuring the time to peak current at voltages between −30 and +30 mV at 37 and 40°C of (D) $Na_v1.1$ WT (■, 37°C, $n = 13$; □, 40°C, $n = 13$), (E) R859H (●, 37°C, $n = 12$; ○, 40°C, $n = 12$), and (F) R865G (▲, 37°C, $n = 10$; △, 40°C, $n = 10$) ion channels. Only WT showed a significant decrease in time to peak current at 40°C. (G and H) Comparison of the time to peak current of $Na_V1.1$ WT, R859H, and R865G at (G) 37°C and (H) 40°C, showing a significant decrease in time to peak current at 37°C but not 40°C. (I–K) The decay of the sodium currents was fitted by a double exponential to obtain fast and slow inactivation time constants of (I) $Na_v1.1$ WT, (J) R859H, and (K) R865G at physiological and febrile temperatures. The R859H mutant showed a small but significant decrease in the fast time constant of inactivation at 40°C compared with 37°C between −30 and −20 mV. (L and M) Comparison of fast and slow inactivation time constants of WT and mutant channels plotted against the membrane potential at (L) 37°C and (M) 40°C, demonstrating decreased speed in fast inactivation time constants between −30 and −20 mV for R859H at 40°C. Data points that significantly differ are indicated as *, $P < 0.05$; **, $P < 0.01$; and †, $P < 0.001$.

voltage dependence of fast inactivation with a double Boltzmann equation, $I = I_1/(1 + \exp((V - V_1 1/2)/k_1)) + I_2/(1 + \exp((V - V_2 1/2)/k_2))$, where V is the variable test or conditioning potential, $V1/2$ are the voltages of half-maximum activation or inactivation, k are slope factors, I_1 and I_2 are the fractional amplitudes of I_{max}, and I_{max} is the normalized maximum amplitude of the sodium current. The entry into and recovery from fast and slow inactivation was analyzed by fitting the data with a double exponential, $I/I_{max} = A_1 \times (1 - \exp(-t/\tau_1)) + A_2 \times (1 - \exp(-t/\tau_2)) + C$, where τ_1 and τ_2 denote the first and second phase of the inactivation time constant, A_1 and A_2 represent the fractional amplitude of each time constant, and C is the level of noninactivating sodium current. Speed of inactivation was evaluated by fitting the decay phase of the sodium current with a double-exponential function, $I/I_{max} = A_1 \times \exp(-t/\tau_1) + A_2 \times \exp(-t/\tau_2) + C$, where the parameters are defined as above. Persistent sodium current was determined by applying a 100-ms depolarizing pulse at voltages −20, −10, and 0 mV from a holding potential of −120 mV. Cells were recorded in the absence and presence of 10 µM tetrodotoxin (TTX; Alomone Labs), and traces were digitally subtracted to obtain persistent current. Next, the average persistent current at the final 10 ms of the depolarizing pulse was normalized to the peak sodium current. Use-dependency was investigated by applying 100 depolarizing test pulses of 2 ms to +15 mV starting from a resting membrane potential of −65 mV at various frequencies (10, 20, 33, 40, 64, 80, 100, 125, and 143 Hz). The peak current of the last pulse was normalized to the peak current generated by the first pulse. The Q_{10} value of sodium current densities measured at −5 mV was calculated using the formula $Q_{10} = (I_{40°C}/I_{37°C})^{(10/(T2-T1))}$, where $I_{37°C}$ and $I_{40°C}$ represent the sodium current densities at the indicated temperatures, and $T1$ and $T2$ are 37 and 40°C, respectively. Voltages are not corrected for liquid junction potentials of 9.9 mV (37°C) and 10 mV (40°C). Data analysis was performed using Clampfit 9.2 (Molecular Devices), Excel (version 2008; Microsoft), KaleidaGraph (version 4.0; Synergy Software), and OriginPro (version 8.0; GE Healthcare) software. Results are presented as mean ± SEM. Statistical analysis was performed using an unpaired Student's t test. A value of $P < 0.05$ was considered significant.

RESULTS

The DS mutant R865G produces reduced peak sodium currents at physiological and febrile temperatures

$Na_v1.1$ WT, R859H, and R865G sodium currents were obtained by applying test pulses ranging from −80 to +90 mV from a holding potential of −120 mV. Fig. 1 (A–F) shows sodium current densities for WT, R859H,

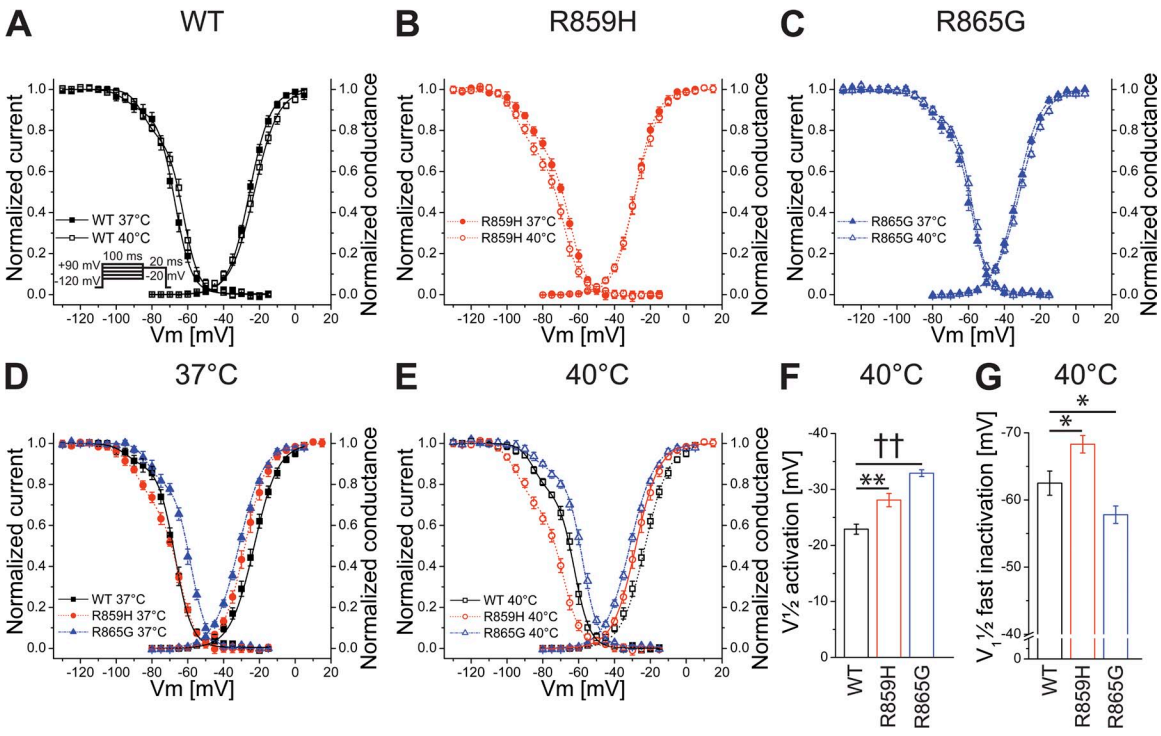

Figure 3. The voltage dependence of activation and inactivation of (A) $Na_v1.1$ WT (■, 37°C; □, 40°C), (B) R859H (●, 37°C; ○, 40°C), and (C) R865G (▲, 37°C; △, 40°C) sodium channels at 37 and 40°C. The number of independent data points for the voltage dependence of activation experiments was: WT 37°C, $n = 13$, and 40°C, $n = 13$; R859H 37°C, $n = 12$, and 40°C, $n = 12$; R865G 37°C, $n = 10$, and 40°C, $n = 10$. The number of independent data points for the voltage dependence of inactivation experiments was: WT 37°C, $n = 10$, and 40°C, $n = 9$; R859H 37°C, $n = 9$, and 40°C, $n = 8$; R865G 37°C, $n = 8$, and 40°C, $n = 9$. (D and E) Comparison of the voltage dependence of activation and inactivation of WT and mutant channels at (D) 37°C and (E) 40°C, and (F and G) the half-maximal values of WT, R859H, and R865G channels of the voltage dependent of (F) activation and (G) fast inactivation at 40°C. The voltage-clamp protocol depicted in A applies to the voltage dependence of inactivation. The protocol used for determining activation can be found in Fig. 1 D. Compared with WT, both mutants showed a gain of function in the voltage dependence of activation at both temperatures. The negative shift in the voltage dependence of inactivation of the GEFS+ mutant indicated decreased channel availability at febrile temperatures, whereas the DS mutant showed a gain of function in the voltage dependence of inactivation at both temperatures. *, $P < 0.05$; **, $P < 0.01$; ††, $P < 0.0001$.

and R865G channels at room temperature (RT), 37°C, and 40°C. When the temperature was raised from 37 to 40°C, WT ion channels gained approximately −50 pA/pF in peak current density, and a similar increase in sodium current density at elevated temperature was also present in the R859H mutant (Fig. 1, A and B). In contrast, the R865G mutation caused no significant increase at 40°C (Fig. 1 C). Compared with WT, R865G showed a trend toward a reduction in sodium current density at physiological temperature and a significant reduction at voltages −10 to 30 mV at 40°C (Fig. 1, E and F). This reduction was not detected at room temperature (Fig. 1 D). Thus, the R865G mutant shows a loss-of-function defect in current density at febrile temperature. We calculated the Q_{10} value of the temperature-dependent current density changes between 37 and 40°C at −5 mV. The Q_{10} value of the R865G mutant (1.17 ± 0.14; t_{21} = 2.58; P = 0.017; n = 10) was significantly lower than WT (2.38 ± 0.40; n = 13) or R859H (2.13 ± 0.32; n = 12) sodium channels, suggesting that the R865G mutant is less temperature dependent than WT.

Time to peak current and speed of inactivation

To determine whether the speed of activation or inactivation plays a role in the reduced current density of the R865G mutant, we analyzed the activation time by measuring the time from the onset to the peak of sodium currents (time to peak current). Fitting the decay phase of the sodium currents with a double-exponential function to obtain the first and second phase of the fast inactivation time constants determined the inactivation rate. Febrile temperatures increased the rate of activation (decreased time to peak current) of WT channels, whereas the speed of inactivation was unaffected (Fig. 2, A, D, and I). The R859H mutant showed similar activation rates at both temperatures, a significant decrease in time constants for the first phase of fast inactivation at 40°C at membrane potentials between −30 and −20 mV and a trend toward increased speed of inactivation for the second phase of fast inactivation at all voltage ranges (Fig. 2, B, E, and J). The kinetics of the R865G mutant were unaffected by febrile temperature (Fig. 2, C, F, and K) and were comparable to the activation rate and speed of inactivation of WT channels at 40°C (Fig. 2, H and M), indicating that neither time to peak nor speed of inactivation contributes to the reduced current density of R865G at elevated temperatures.

Voltage dependence of activation is not temperature sensitive

Next, we analyzed the voltage dependence of activation. Febrile temperature caused a depolarizing shift in the voltage dependence of activation of WT ion channels (Fig. 3 A and Table 1). The half-maximal activation (V1/2) at 40°C of R859H was similar to 37°C, whereas the R865G mutant showed a significant depolarizing shift in the voltage dependence of activation at 40°C (Fig. 3, B and C, and Table 1). Compared with WT, however, there was a significant hyperpolarized shift in the voltage dependence of activation of R859H (V1/2

TABLE 1

Biophysical parameters of $Na_v1.1$ WT, R859H, and R865G sodium ion channels measured at 37 and 40°C

Gating process	Parameter	$Na_v1.1$ WT 37°C	$Na_v1.1$ WT 40°C	R859H 37°C	R859H 40°C	R865G 37°C	R865G 40°C
Activation	V1/2 (mV)	−25.5 ± 0.6	−22.9 ± 0.9[a]	−28.3 ± 1.0	−28.1 ± 1.2	−32.9 ± 0.6	−31.4 ± 0.6[b]
	k	5.9 ± 0.3	6.7 ± 0.3[a]	6.0 ± 0.3	6.3 ± 0.4	6.5 ± 0.2	7.0 ± 0.2
	n	13	13	12	12	10	10
Fast inactivation	$V_1$1/2 (mV)	−67.2 ± 1.0	−62.5 ± 1.8[a]	−64.7 ± 1.3	−68.3 ± 1.3[a]	−58.4 ± 1.4	−57.8 ± 1.3
	k_1	4.7 ± 0.3	4.4 ± 0.1	4.9 ± 0.3	4.9 ± 0.4	4.6 ± 0.5	4.3 ± 0.1
	A_1	0.72 ± 0.03	0.73 ± 0.01	0.64 ± 0.02	0.69 ± 0.02[a]	0.75 ± 0.03	0.74 ± 0.03
	$V_2$1/2 (mV)	−94.7 ± 2.2	−85.4 ± 2.3[a]	−87.8 ± 2.3	−94.3 ± 1.9	−82.9 ± 2.8	−83.9 ± 2.5
	k_2	4.4 ± 0.8	3.9 ± 0.7	5.8 ± 0.9	5.1 ± 0.9	3.5 ± 0.8	6.3 ± 1.3[a]
	A_2	0.28 ± 0.04	0.27 ± 0.01	0.35 ± 0.02	0.32 ± 0.02	0.25 ± 0.03	0.26 ± 0.03
	n	10	9	9	8	8	9
Recovery from inactivation	τ_1 (ms)	10.1 ± 2.10	8.80 ± 1.40	5.90 ± 1.20	23.8 ± 8.80[c]	26.8 ± 5.30	13.2 ± 3.36[a]
	A_1	0.32 ± 0.04	0.48 ± 0.07[a]	0.18 ± 0.03	0.33 ± 0.07[a]	0.48 ± 0.08	0.30 ± 0.05[a]
	τ_2 (ms)	46.3 ± 4.50	47.7 ± 6.30	175 ± 14.8	141 ± 13.9[a]	128 ± 20.8	53.1 ± 7.10[d]
	A_2	0.47 ± 0.04	0.33 ± 0.07	0.68 ± 0.04	0.49 ± 0.07[a]	0.36 ± 0.07	0.57 ± 0.05[a]
	n	13	9	12	12	10	9

Fast gating parameters of the WT $Na_v1.1$ channel and the two mutants R859H and R865G at 37 and 40°C. Shown are the voltage dependence of activation and inactivation and the recovery from inactivation. Ion channel fast gating parameters at 40°C that significantly differ from the values obtained at 37°C are indicated as follows:

[a]P < 0.05.

[b]P < 0.0001.

[c]P < 0.001.

[d]P < 0.01.

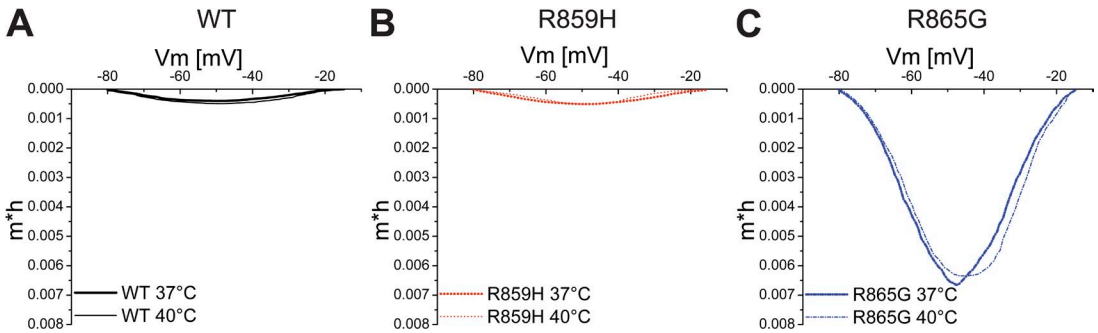

Figure 4. Window currents produced by (A) $Na_v1.1$ WT, (B) R859H, and (C) R865G channels at 37 and 40°C. The voltage dependence and amplitude of the window current was estimated by plotting the product of the average fractional availability for steady-state activation (m) and inactivation (h) curves (obtained from Fig. 3, A–C). The resultant values show the fraction of active WT, R859H, or R865G sodium channels as a function of the membrane potential. The DS mutant R865G clearly shows an enlarged window current compared with $Na_v1.1$ WT and R859H currents.

37°C = −28.3 ± 1.0, t_{23} = 2.45, P = 0.02, and n = 12; V1/2 40°C = −28.1 ± 1.2, t_{23} = 3.41, P = 0.002, and n = 12) and R865G (V1/2 37°C = −32.9 ± 0.6, t_{21} = 8.02, P < 0.0001, and n = 10; V1/2 40°C = −31.4 ± 0.6, t_{23} = 7.09, P < 0.0001, and n = 10) at both temperatures, albeit more prominent for the DS mutation (Fig. 3, D–F). On the other hand, the V1/2 at 37 and 40°C of WT, R859H, and R865G is similar to the values obtained at room temperature ($Na_v1.1$ WT: −23.1 ± 1.1 mV; R859H: −27.1 ± 0.6 mV; R865G: −31.2 ± 1.1 mV; Volkers et al., 2011), indicating that increased temperatures do not affect the activation gating of the $Na_v1.1$ WT ion channel and mutants.

The GEFS+ mutant R859H shows febrile temperature–induced decrease in voltage-dependent channel availability

Subsequently, we investigated steady-state inactivation by applying a series of depolarizing conditioning pulses in the voltage range of −140 to 0 mV starting from a holding potential of −120 mV, immediately followed by a depolarizing test pulse of −20 mV. Steady-state channel inactivation was best fitted by a double Boltzmann equation. When temperature was raised to 40°C, WT channels showed an increase in channel availability (Fig. 3 A and Table 1). Opposite results were obtained for the R859H mutant, which showed a significant hyperpolarized shift in the voltage dependence of inactivation at elevated temperatures (Fig. 3 B and Table 1). Furthermore, the contribution of the more negative portion of the Boltzmann curve (A_2) for R859H was significantly increased compared with WT channels at 37°C (A_2 R859H = 0.35 ± 0.02; t_{17} = 2.11; P = 0.049; n = 9) (Table 1). The temperature-dependent negative shift in the steady-state inactivation of sodium ion channels harboring the R859H mutation suggests that fever leads to a decrease in channel availability (Fig. 3, B, E, and G).

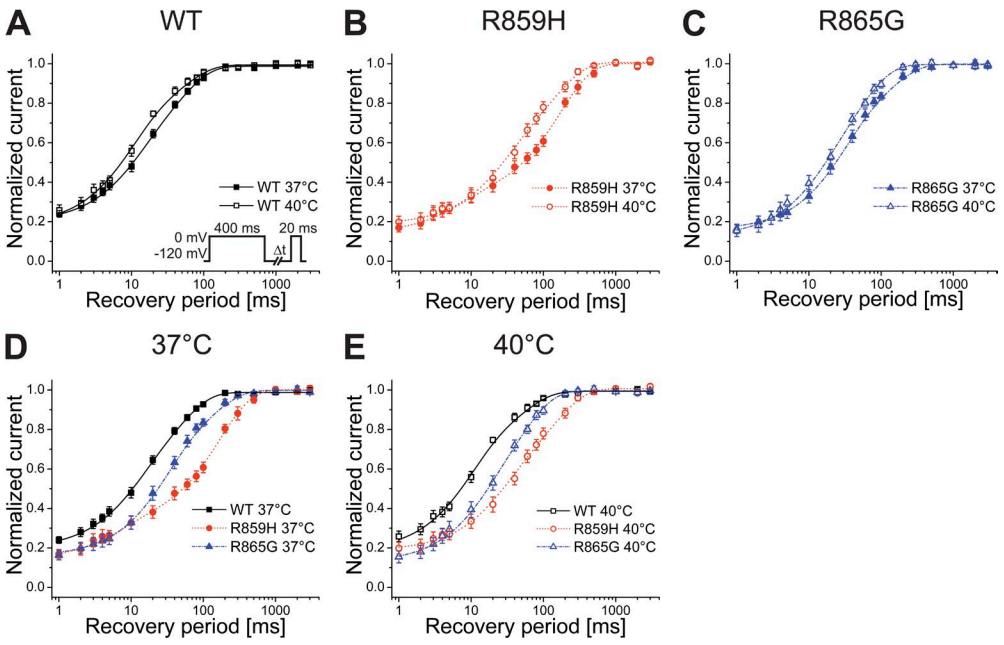

Figure 5. Time-dependent recovery from inactivation at 37 and 40°C of (A) $Na_v1.1$ WT (■, 37°C, n = 13; □, 40°C, n = 9), (B) R859H (●, 37°C, n = 12; ○, 40°C, n = 12), and (C) R865G (▲, 37°C, n = 10; △, 40°C, n = 9) sodium ion channels was assessed using the two-pulse protocol shown in the inset of A. Peak currents during the test pulse were normalized to the peak currents generated by the conditioning pulse and plotted against the recovery time. (D and E) Comparison of the recovery from inactivation of WT and mutant channels at (D) 37°C and (E) 40°C. Significant slowing in recovery from inactivation at 37 and 40°C was observed for both mutants (see also Table 1).

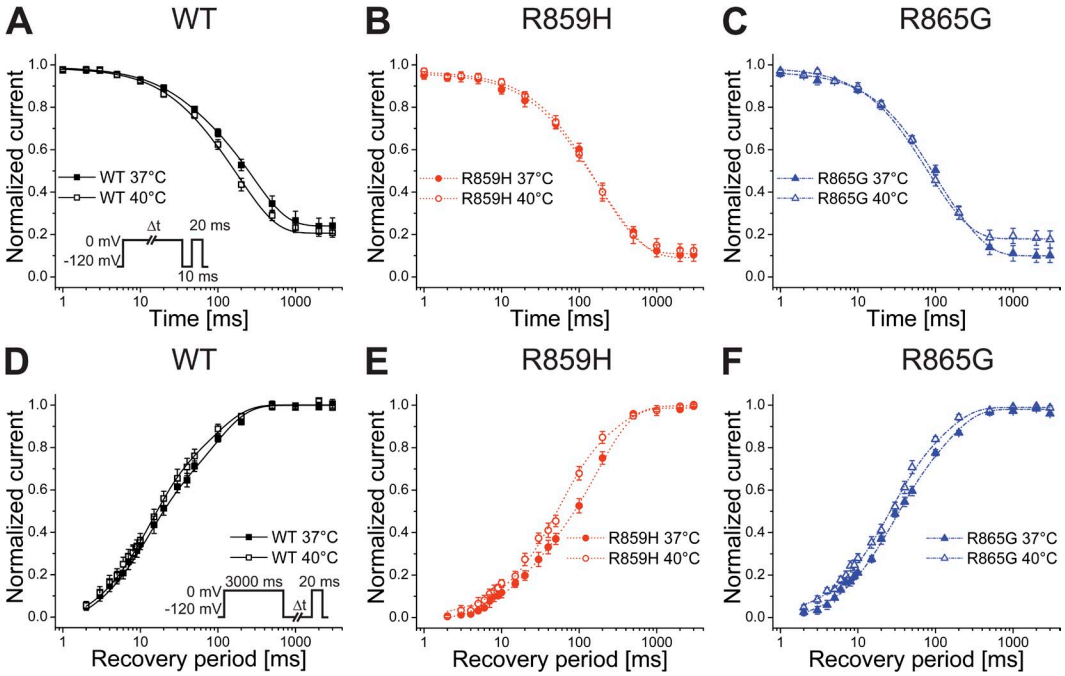

Figure 6. Biophysical slow gating characteristics of $Na_v1.1$ WT, R859H, and R865G channels. (A–C) Time-dependent entry into inactivation of (A) $Na_v1.1$ WT (■, 37°C, $n = 8$; □, 40°C, $n = 10$), (B) R859H (●, 37°C, $n = 9$; ○, 40°C, $n = 12$), and (C) R865G (▲, 37°C, $n = 7$; △, 40°C, $n = 10$). Sodium channels were inactivated by a depolarizing pulse to 0 mV with varying duration between 1 and 3,000 ms and allowed to recover from fast inactivation for 10 ms, followed by a depolarizing test pulse to 0 mV. (D–F) Recovery from slow inactivation of (D) $Na_v1.1$ WT (37°C, $n = 10$; 40°C, $n = 10$), (E) R859H (37°C, $n = 8$; 40°C, $n = 9$), and (F) R865G (37°C, $n = 7$; 40°C, $n = 10$) measured at 37 and 40°C. Sodium channels were inactivated by a 3,000-ms depolarizing pulse to 0 mV and allowed to recover for increasing time periods at −120 mV, before giving a 20-ms test pulse at 0 mV. Peak currents obtained from the test pulses were normalized to the peak currents obtained from the conditioning pulse and plotted against the recovery time.

In contrast, elevated temperatures did not affect the voltage dependence of inactivation of the R865G mutant (Fig. 3 C and Table 1). However, the R865G mutant at 37 and 40°C revealed an increase in the voltage dependence of channel availability compared with WT channels ($V_1 1/2$ 37°C = −58.4 ± 1.4, $t_{16} = -5.45$, $P < 0.0001$, and $n = 9$; $V_1 1/2$ 40°C = −57.8 ± 1.3, $t_{16} = -2.14$, $P < 0.048$, and $n = 9$) (Fig. 3, D, E, and G), a feature that was not observed at room temperature (Volkers et al., 2011).

R865G exhibits increased window current

The steady-state activation and inactivation curves showed an overlap, indicating that a window current was present. Compared with WT, the window current of R865G was enlarged because of the shifts in the voltage dependence of activation and inactivation (Fig. 3, A, C, F, and G). We have therefore analyzed changes in the window current in more detail. The size of the window current produced by WT, R859H, and R865G channels was calculated as the product of the average steady state of activation (m) and inactivation (h). These resultant products are a measure of the probability of incompletely inactivated or deactivated sodium channels to open and were plotted against the membrane potential. The size of the window current of R865G was increased >10-fold at both 37 and 40°C compared with WT (Fig. 4, A–C). This increased window current results in an increase in channel function, especially when the membrane potential is near firing threshold, which could lead to enhanced excitability.

Recovery from inactivation is delayed in both mutants

Febrile temperatures accelerated the recovery from inactivation of both WT and mutant channels. However, this effect was less pronounced in both mutants (Fig. 5, A–E, and Table 1). At 37°C, cells expressing R859H had a significantly smaller fraction of channels recovering from the fast inactivation component (A_1) and a larger population recovering from the slower inactivation (A_2) compared with WT ($A_1 = 0.48 \pm 0.07$, $t_{23} = 2.82$, $P = 0.01$, and $n = 12$; $A_2 = 0.68 \pm 0.04$, $t_{23} = -3.96$, $P = 0.0006$, and $n = 12$) (Table 1). In addition, there was a significant slowing in recovery from inactivation, as was evident by a larger time constant (τ_2) of recovery ($\tau_2 = 128 \pm 20.8$; $t_{23} = -8.63$; $P < 0.0001$; $n = 12$). At 40°C, the recovery from inactivation of R859H is accelerated but still significantly slower compared with WT channels (τ_1 R859H = 23.8 ± 8.80; $t_{19} = -3.23$; $P = 0.004$; $n = 9$) (Fig. 5 E). The R865G mutation also caused an overall slowing in recovery from inactivation at 37 and 40°C, as shown by the larger time constants τ_1 (τ_1 $t_{17} = 2.11$; $P = 0.049$) (Table 1 and

TABLE 2

Biophysical parameters of slow inactivation of $Na_v1.1$ WT, R859H, and R865G sodium ion channels measured at 37 and 40°C

Gating process	Parameter	$Na_v1.1$ WT 37°C	$Na_v1.1$ WT 40°C	R859H 37°C	R859H 40°C	R865G 37°C	R865G 40°C
Entry into slow inactivation	τ_1 (ms)	35.8 ± 9.30	42.6 ± 9.80	64.3 ± 16.2	69.3 ± 14.3	50.2 ± 10.8	36.4 ± 9.00
	A_1	0.14 ± 0.03	0.16 ± 0.04	0.29 ± 0.06	0.24 ± 0.06	0.32 ± 0.08	0.25 ± 0.08
	τ_2 (ms)	290 ± 26.3	217 ± 19.8[a]	302 ± 28.3	216 ± 26.5[a]	196 ± 23.1	122 ± 9.50[a]
	A_2	0.61 ± 0.05	0.61 ± 0.04	0.58 ± 0.08	0.62 ± 0.06	0.55 ± 0.09	0.56 ± 0.07
	$I_{residual}$ (%)	26 ± 4	22 ± 2	14 ± 3	14 ± 3	13 ± 4	19 ± 4
	n	8	10	9	12	9	10
Slow inactivation	V1/2 (mV)	−54.3 ± 1.0	−57.9 ± 1.1[a]	−56.3 ± 1.2	−59.3 ± 0.7[a]	−64.3 ± 0.9	−65.6 ± 0.8
	k	6.9 ± 0.4	6.9 ± 0.5	7.5 ± 0.3	7.6 ± 0.4	6.6 ± 0.3	6.3 ± 0.5
	n	11	10	10	7	7	7
Recovery from slow inactivation	τ_1 (ms)	11.2 ± 1.80	11.8 ± 1.90	18.7 ± 7.70	25.4 ± 5.10	22.5 ± 2.80	21.3 ± 3.9
	A_1	0.57 ± 0.06	0.65 ± 0.07	0.23 ± 0.03	0.31 ± 0.07	0.52 ± 0.07	0.59 ± 0.07
	τ_2 (ms)	90.7 ± 8.80	86.0 ± 14.6	178 ± 29.2	131 ± 13.8[a]	124 ± 8.00	111 ± 17.8
	A_2	0.49 ± 0.05	0.41 ± 0.07	0.79 ± 0.02	0.68 ± 0.08	0.48 ± 0.06	0.40 ± 0.07
	n	10	10	8	9	7	10

Slow gating parameters of the WT $Na_v1.1$ channel and the two mutants R859H and R865G at 37 and 40°C. Shown are the entry into inactivation and the voltage dependence of and the recovery from slow inactivation. Ion channel slow gating parameters at 40°C that significantly differ from the values obtained at 37°C are indicated as follows:
[a]$P < 0.05$.

Fig. 5 D). At 40°C, a smaller R865G channel population was recovering from the fast inactivation component (A_1 t_{17} = 2.11; P = 0.049) and a significant larger ion channel population was present in the second inactivation status (A_2 t_{17} = 3.24; P = 0.048) (Table 1). In summary, these results show that both mutants exhibited a slowing in recovery from inactivation at both temperatures, with the largest delay observed for R859H (Fig. 5, A–E).

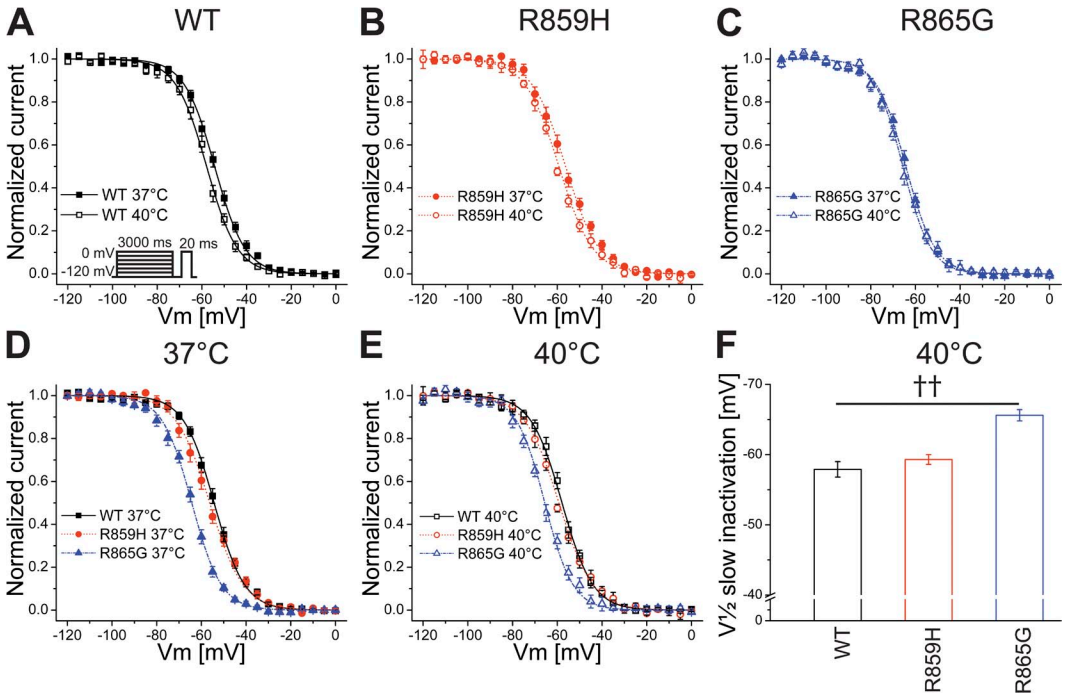

Figure 7. Steady-state voltage dependence of slow inactivation of (A) $Na_v1.1$ WT (■, 37°C, *n* = 11; □, 40°C, *n* = 10), (B) R859H (●, 37°C, *n* = 10; ○, 40°C, *n* = 7), and (C) R865G (▲, 37°C, *n* = 7; △, 40°C, *n* = 7) at 37 and 40°C was assessed by applying depolarizing conditioning pulses of 3 s, starting from −120 to 0 mV, with 5-mV increments. Cells were allowed to recover from fast inactivation for 10 ms before applying a 20-ms depolarizing test pulse to 0 mV. Peak currents of the test pulse were normalized to the peak currents obtained from the conditioning pulse and plotted against the duration of the conditioning pulse. (D and E) Comparison of the voltage dependence of slow inactivation of WT and mutant channels at (D) 37°C and (E) 40°C. (F) The half-maximal values of the voltage dependence of slow inactivation of WT, R859H, and R865G channels at 40°C show a significant hyperpolarized shift for the R865G mutant (††, $P < 0.0001$). WT and the R859H mutant showed a significant hyperpolarized shift in voltage dependence of slow inactivation at 40°C (see also Table 2).

R859H and R865G mutants have gating defects in slow inactivation

Slow inactivation is a process distinct from fast inactivation. This independent process is functionally relevant for setting the fractional availability of the sodium channel population at voltages around the resting membrane potential or in response to prolonged bursts of action potentials.

The entry into inactivation was analyzed by fitting the data to a double-exponential function (Fig. 6, A–C). Increased temperatures accelerated the entry into inactivation of WT, R859H, and R865G channels, which is evident by decreased time constants τ_2 (Table 2). Compared with WT ion channels, at 37°C, both mutants have a larger inactivating ion channel population in the first time fraction (A_1) (A_1 R859H = 0.29 ± 0.06, t_{15} = 2.24, P = 0.04, and n = 9; A_1 R865G = 0.32 ± 0.08, t_{15} = 2.15, P = 0.049, and n = 9) than WT ion channels (Fig. 6, A–C, and Table 2). At both temperatures, R859H had a larger ion channel population that entered into a slow inactivation state compared with WT, as evident by the smaller value of the residual current ($I_{residual}$ 37°C = 14 ± 3, t_{15} = 2.89, P = 0.01, and n = 9; $I_{residual}$ 40°C = 14 ± 3, t_{15} = 2.10, P = 0.048, and n = 12) (Fig. 5, A and B, and Table 2). At 40°C, the $I_{residual}$ of R865G is similar to WT (t_{18} = 0.57; P = 0.57; n = 10) (Table 2). Compared with WT, the R865G mutant showed an acceleration of entry into steady-state inactivation (τ_2) at both temperatures (τ_2 37°C: t_{15} = 2.69, P = 0.02, and n = 9; τ_2 40°C: t_{18} = 4.34, P = 0.0004, and n = 10).

Fig. 6 (D–F) shows the recovery from slow inactivation for WT, R859H, and R865G. Compared with WT, both mutations caused a significant slowing in recovery from slow inactivation at both temperatures (Fig. 6, D–F, and Table 2), albeit more prominent for R859H.

At 40°C, both WT and R859H channels showed a hyperpolarized shift in the voltage dependence of steady-state slow inactivation (Fig. 7, A and B). The steady-state slow inactivation of R859H channels at both temperatures was comparable to WT, whereas the R865G mutation caused a hyperpolarized shift in the V1/2 of −10 and −7.7 mV at 37 and 40°C, respectively (V1/2 37°C = −64.3 ± 0.9, t_{16} = 6.96, P < 0.0001, and n = 7; V1/2 40°C = −65.6 ± 0.8, t_{15} = 5.26, P < 0.0001, and n = 10) (Fig. 7, A–F, and Table 2).

R859H and R865G exhibit divergent use-dependency at elevated temperatures

We tested the use-dependent behavior of WT and mutant ion channels by applying a train of 2-ms depolarizing test pulses at various frequencies to mimic repetitive action potential firing. The use-dependency was analyzed by normalizing the peak sodium currents during the last test pulse to currents generated during the first pulse (Fig. 8). When temperature was increased to 40°C, WT ion channels showed a trend toward decreased use-dependent decay in sodium currents (Fig. 8 A). In contrast, the R859H mutation caused a significant increase in use-dependence in the frequency range of 64–143 Hz (Fig. 8 B), whereas R865G showed

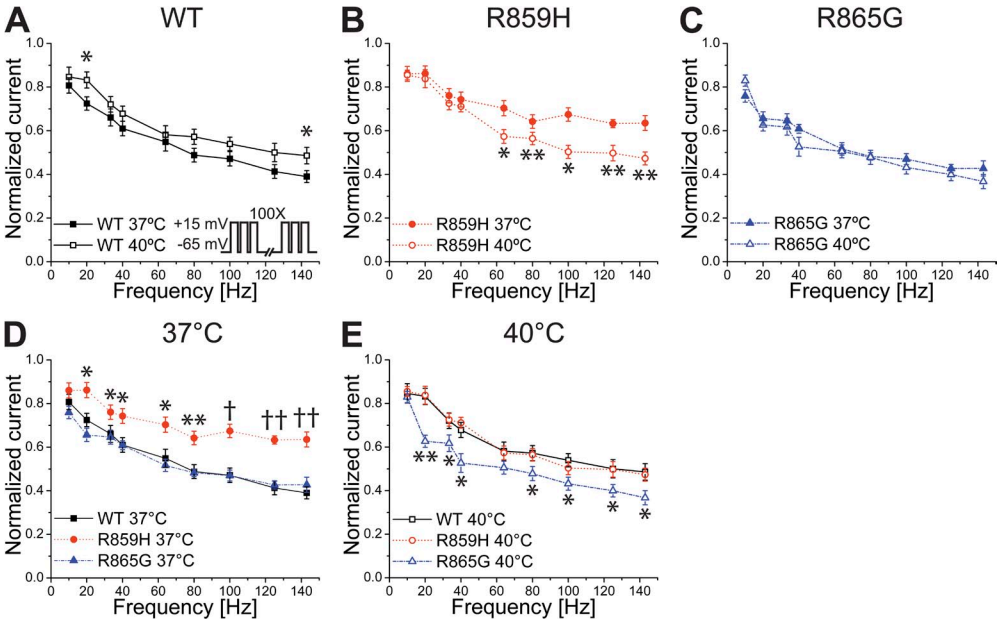

Figure 8. Use-dependent channel availability of (A) $Na_v1.1$ WT (■, 37°C, n = 10; □, 40°C, n = 7), (B) R859H (●, 37°C, n = 7; ○, 40°C, n = 6), and (C) R865G (▲, 37°C, n = 7; △, 40°C, n = 8) channels at 37 and 40°C. Cells were given a train of 100 depolarizing pulses of 2 ms from a holding membrane potential of −65 to +15 mV at various frequencies. Peak sodium currents of the last pulse (100th) were normalized to the peak currents generated at the first pulse. WT channels showed a slight decreased use-dependency at 40°C. In contrast, the GEFS+ mutant R859H showed a significant increase in use-dependency at a frequency range of 64–143 Hz, whereas the use-dependency of R865G was unaffected by febrile temperatures. (D and E) Comparison of the use-dependency of $Na_v1.1$ WT, R859H, and R865G at (D) 37°C and (E) 40°C. At 37°C, WT and R865G showed similar use-dependencies, whereas the use-dependency of R859H was decreased. At 40°C, WT and R859H channels had similar use-dependencies, and the use-dependency of the R865G mutant at most frequencies was significantly increased. Values significantly different between WT and mutant ion channels (D and E) or between measurements at 37 and 40°C (A–C) are as follows: *, P < 0.05; **, P < 0.01; †, P < 0.001; ††, P < 0.0001.

a similar use-dependent behavior at both temperatures (Fig. 8 C).

At 37°C, the use-dependency of R859H was significantly less use-dependent than WT and R865G, whereas R865G was similar as WT (Fig. 8 D). At 40°C, R859H channels showed similar use-dependency as WT channels. The R865G mutation caused an increase in use-dependent behavior at frequencies of 20–40 Hz and 80–143 Hz compared with WT sodium channels (Fig. 8 E).

Absence of increased persistent current in R859H and R865G mutants

In our previous characterization at room temperature, both mutants exhibited a significant increase in persistent current (Volkers et al., 2011). Because persistent current is rather common in GEFS+ and DS mutant channels at room temperature (Lossin et al., 2002; Rhodes et al., 2004), we examined the persistent current of these mutant channels at physiological and febrile temperatures. In contrast to our previous findings, both mutants had comparable small persistent currents as WT channels at elevated temperatures (Fig. 9, A–C).

DISCUSSION

Molecular defects in $Na_v1.X$ ion channels have been reported in association with temperature-sensitive disorders such as heat-induced myotonia and cold-induced paramyotonia linked to $Na_v1.4$ mutations; Brugada syndrome associated with $Na_v1.5$ mutations; and erythromelalgia, a disabling chronic pain disorder associated with mutations in the $Na_v1.7$ ion channel. $Na_v1.4$, $Na_v1.5$, and $Na_v1.7$ sodium ion channels are thermosensitive, and mutations in these ion channel proteins can alter the temperature-dependent gating of the channel (Dumaine et al., 1999; Han et al., 2007; Webb and Cannon, 2008; Carle et al., 2009; Samani et al., 2009).

Fever-induced seizures are common in GEFS+ and DS subjects, and GEFS+ and DS mouse models showed increased seizure susceptibility at elevated body temperatures (Oakley et al., 2009; Martin et al., 2010). The physiological mechanisms behind the temperature-dependent reduced seizure threshold are unclear. Reversible temperature-dependent trafficking defects in the $GABA_A$ γ2-subunit receptor—associated with GEFS+—have been reported, which suggest that accelerated endocytosis could be caused by an abnormal folding of the receptor protein at elevated temperatures (Kang et al., 2006). Abnormal folding of the $Na_v1.1$ ion channel has also been shown for two *SCN1A* mutations at room temperature (Rusconi et al., 2007, 2009). This suggests that a lowered inhibition by GABAergic interneurons at febrile temperatures is a contributing factor to febrile seizures in individuals harboring a $Na_v1.1$ mutation. DS *Scn1a* mouse models already show drastically reduced sodium currents in GABAergic interneurons that cause action potential attenuation during repetitive firing (Yu et al., 2006; Ogiwara et al., 2007). In addition, *Scn1a* heterozygote animals also show markedly different effects depending on the genetic background, with one strain having a more severe phenotype compared with other strains (Yu et al., 2006). Also, truncation mutations in *SCN1A* in patients can lead to febrile seizures or GEFS+ instead of DS (Gennaro et al., 2003; Yu et al., 2010). These observations reflect the role of genetic background or modifier genes in the phenotypic outcome of DS patients. Additionally, the role of acute fever in triggering the seizure remains to be clarified.

Previous work on the R859H (GEFS+) and R865G (DS) mutant channels studied at room temperature demonstrated a gain of function in the voltage dependence of activation and a loss of function in recovery of fast inactivation for both mutants (Volkers et al., 2011). In addition, the R859H mutant also showed a loss of function in the voltage dependence and speed of inactivation. The current densities of I_{Na} carried by both mutated channels were comparable to WT. Although the slow inactivation behavior of these channels was not investigated, the data recorded at room temperature suggest only small gating defects for the R865G mutant that are insufficient to explain the severe phenotype of this patient. Therefore, in this study, we characterized the

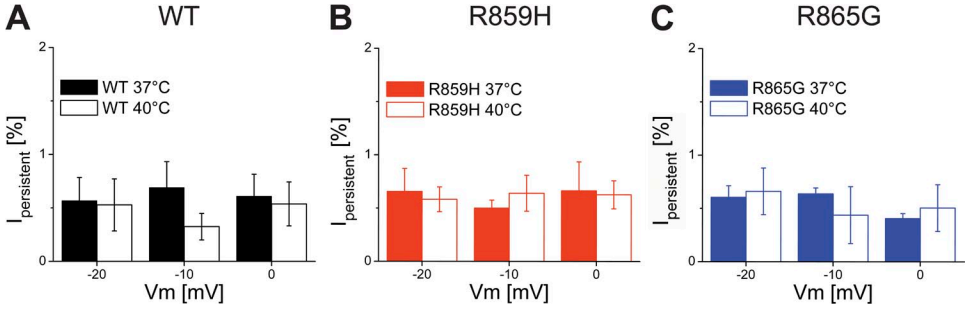

Figure 9. Persistent current of (A) $Na_v1.1$ WT (37 and 40°C, $n = 4$), (B) R859H (37 and 40°C, $n = 4$), and (C) R865G (37 and 40°C, $n = 5$) ion channels measured at 37 and 40°C. Cells were given 100-ms depolarizing test pulses to −20, −10, and 0 mV from a holding potential of −120 mV with and without TTX in the bath solution. Sodium currents recorded in the absence of TTX were digitally subtracted from currents obtained in the presence of TTX. The amplitude of the persistent current was measured at the last 10 ms of the 100-ms depolarizing pulse and normalized to the peak sodium current. No significant differences between $Na_v1.1$ WT and R859H or R865G mutants were found.

biophysical behavior of these two mutants, R859H and R865G, at physiological and febrile temperature to mimic the pathophysiological condition at which these epileptic seizures are triggered.

Physiological and febrile temperatures (37 and 40°C) unmasked a depolarized shift in the voltage dependence of inactivation (gain of function) of the R865G channel and a significant decrease in current density compared with WT channels, which was not detected previously at room temperature (Volkers et al., 2011). Opposite results were obtained for R859H channels, where loss of function in voltage-dependent channel availability found at room temperature was virtually abolished at 37°C but unmasked again at 40°C. In addition, the reduced speed of inactivation detected at room temperature was abolished at 37°C and increased at 40°C at a range of −30 to −20 mV. These results emphasize that caution should be used when extrapolating ion channel gating properties obtained at room temperature to 37 or 40°C using a single scale factor. Moreover, our results underline the need of electrophysiological measurements at physiological and febrile temperatures to gather a better insight in the biophysical behavior of $Na_v1.1$ WT and mutated ion channels.

At room temperature, the R859H and R865G mutations caused an enlarged persistent current (Volkers et al., 2011). Interestingly, this increase in persistent current was abolished completely at 37 and 40°C. This suggests that the stabilization of the inactivation gate of $Na_v1.1$ channels is highly temperature sensitive and that these mutations hamper complete channel inactivation at lower temperatures. Whether the increased persistent sodium currents measured in other mutants associated with GEFS+ and DS (Lossin et al., 2002; Rhodes et al., 2004) can still be relevant at physiological and febrile temperatures remains to be determined.

Compared with WT and R859H channels, R865G shows a >10-fold increase in window current at both temperatures. The window current occurs at a small range of voltages where sodium ion channels activate and inactivate incompletely. This activity can play an important role in the excitability of a neuron, and an increase in window current is predicted to increase channel function. After correction of liquid junction potentials of the patch pipettes (37°C = 9.9 mV; 40°C = 10 mV), the maximal window current is in range of the resting membrane potential of a neuron (approximately −60 mV). This could produce neuronal hyperexcitability by reducing the threshold for initiating action potential firing in an inhibitory neuron that expresses R865G mutant sodium channels. However, the significant window current observed in the DS mutant may depolarize the membrane and/or increase intracellular Na^+ to the point of inducing depolarized block of action potential firing or alterations in action potential shape. This would reflect enhanced steady-state inactivation of R865G sodium channels and/or reduce the ionic driving force for Na^+ compared with WT neurons. Reduced excitability of GABAergic interneurons has been observed in brain slices and dissociated GABAergic interneurons of the *Scn1a*$^{+/-}$ DS mouse model (Yu et al., 2006; Ogiwara et al., 2007).

The voltage dependence of fast inactivation at 37°C revealed two distinct gating processes in $Na_v1.1$ WT and mutant ion channels. The inactivation process present at a more negative voltage range is maybe not very significant because of the hyperpolarized range at which it occurs (Table 1; see $V_21/2$). Interestingly, the voltage dependence of fast inactivation of WT $Na_v1.4$, $Na_v1.5$, and $Na_v1.7$ sodium channels at elevated temperatures shows only one inactivation process (Han et al., 2007; Carle et al., 2009; Samani et al., 2009). This could indicate that the temperature-dependent gating characteristics of $Na_v1.1$ WT ion channels differ between sodium ion channel isoforms.

A DS-like phenotype can be caused by decreased sodium currents in GABAergic inhibitory interneurons, as shown in *Scn1a*$^{+/-}$ DS mouse models (Yu et al., 2006; Ogiwara et al., 2007). In our experiments, the DS mutant R865G also showed an acute reduction in current density at a febrile temperature, although the I_{Na} reduction is not as complete compared with the knockout models. Nevertheless, the reduced neuronal inhibition could contribute to the epileptic severity in DS subjects harboring an R865G mutation. In contrast, at febrile temperatures, the WT sodium currents increase in magnitude and channel availability increases in parallel during repetitive stimulation (gain of function), both of which predict increased GABAergic inhibition and seizure suppression. This divergence in the inhibitory drive of the GABAergic network for WT versus R865G could inform as to the susceptibility of DS patients to febrile convulsions.

In summary, our study indicates that febrile temperatures differentially change the gating of WT and mutated $Na_v1.1$ channels. For the GEFS+ mutant (R859H), we found a temperature-dependent loss of function in the voltage dependence of inactivation and a use-dependent decrease in channel availability during repetitive firing at 40°C. We hypothesize that the decreased voltage-dependent channel availability in combination with an increased use-dependency contributes to the development of febrile seizures in GEFS+ patients harboring a R859H mutation. In the DS mutant R865G, despite the gain of function in the voltage dependence of activation and inactivation at 37 and 40°C, febrile temperatures reduced peak sodium currents and increased use-dependency compared with WT. These data suggest that fever-induced gating defects in combination with the biophysical ion channel alterations at elevated temperatures could contribute to the phenotypic outcome in DS patients with a R865G mutation. In

addition, the faster entry into the slow inactivation state in combination with a loss of function in the voltage dependence of the slow inactivation of R865G at febrile temperatures suggests that prolonged membrane depolarization can ultimately lead to membrane inexcitability in GABAergic inhibitory neurons expressing this mutant, and could explain the severe outcome in this DS subject. The experimental approaches used in this study represent a simplified disease model, and extending these findings to a neuronal or in vivo system is a necessary progression. Indeed, the extensive characterization of the GEFS+ $Na_v1.1$ mutant channel (R1648H) has used a variety of expression systems as well as a transgenic mouse model to measure different or even opposing gating defects (Spampanato et al., 2001; Lossin et al., 2002; Tang et al., 2009). In contrast, the gating defects of N1417H-mutated $Na_v1.1$ channels reported using HEK cells were confirmed in GABAergic interneurons of rats carrying this mutation (Mashimo et al., 2010). These reports highlight the important role played by cellular background, including accessory proteins, compensatory mechanisms, and channel trafficking. Future studies characterizing R865H and R865G, as well as other mutant $Na_v1.1$ channels, in neuronal networks and animal models are necessary to determine how our observations generalize to *SCN1A* epileptic syndromes.

This work was supported by "Ter Meulen Fund," Royal Netherlands Academy of Arts and Sciences (to L. Volkers); The Netherlands Organization of Scientific Research and Development (ZonMW; grant 917.66.315 to B.P.C. Koeleman); and the National Epilepsy Fund of The Netherlands (grant NEF 07-21 to M.J.A. van Kempen). The authors declare no competing financial interests.

Lawrence G. Palmer served as editor.

Submitted: 5 June 2013
Accepted: 17 October 2013

REFERENCES

Amin, A.S., L.J. Herfst, B.P. Delisle, C.A. Klemens, M.B. Rook, C.R. Bezzina, H.A. Underkofler, K.M. Holzem, J.M. Ruijter, H.L. Tan, et al. 2008. Fever-induced QTc prolongation and ventricular arrhythmias in individuals with type 2 congenital long QT syndrome. *J. Clin. Invest.* 118:2552–2561.

Carle, T., E. Fournier, D. Sternberg, B. Fontaine, and N. Tabti. 2009. Cold-induced disruption of Na^+ channel slow inactivation underlies paralysis in highly thermosensitive paramyotonia. *J. Physiol.* 587:1705–1714. http://dx.doi.org/10.1113/jphysiol.2008.165787

Catterall, W.A., F. Kalume, and J.C. Oakley. 2010. NaV1.1 channels and epilepsy. *J. Physiol.* 588:1849–1859. http://dx.doi.org/10.1113/jphysiol.2010.187484

Claes, L.R., B. Ceulemans, D. Audenaert, K. Smets, A. Löfgren, J. Del-Favero, S. Ala-Mello, L. Basel-Vanagaite, B. Plecko, S. Raskin, et al. 2003. De novo *SCN1A* mutations are a major cause of severe myoclonic epilepsy of infancy. *Hum. Mutat.* 21:615–621. http://dx.doi.org/10.1002/humu.10217

Claes, L.R., L. Deprez, A. Suls, J. Baets, K. Smets, T. Van Dyck, T. Deconinck, A. Jordanova, and P. De Jonghe. 2009. The *SCN1A* variant database: a novel research and diagnostic tool. *Hum. Mutat.* 30:E904–E920. http://dx.doi.org/10.1002/humu.21083

Deprez, L., A. Jansen, and P. De Jonghe. 2009. Genetics of epilepsy syndromes starting in the first year of life. *Neurology.* 72:273–281. http://dx.doi.org/10.1212/01.wnl.0000339494.76377.d6

Dumaine, R., J.A. Towbin, P. Brugada, M. Vatta, D.V. Nesterenko, V.V. Nesterenko, J. Brugada, R. Brugada, and C. Antzelevitch. 1999. Ionic mechanisms responsible for the electrocardiographic phenotype of the Brugada syndrome are temperature dependent. *Circ. Res.* 85:803–809. http://dx.doi.org/10.1161/01.RES.85.9.803

Escayg, A., B.T. MacDonald, M.H. Meisler, S. Baulac, G. Huberfeld, I. An-Gourfinkel, A. Brice, E. LeGuern, B. Moulard, D. Chaigne, et al. 2000. Mutations of *SCN1A*, encoding a neuronal sodium channel, in two families with GEFS+2. *Nat. Genet.* 24:343–345. http://dx.doi.org/10.1038/74159

Gennaro, E., P. Veggiotti, M. Malacarne, F. Madia, M. Cecconi, S. Cardinali, A. Cassetti, I. Cecconi, E. Bertini, A. Bianchi, et al. 2003. Familial severe myoclonic epilepsy of infancy: truncation of Nav1.1 and genetic heterogeneity. *Epileptic Disord.* 5:21–25.

Han, C., A. Lampert, A.M. Rush, S.D. Dib-Hajj, X. Wang, Y. Yang, and S.G. Waxman. 2007. Temperature dependence of erythromelalgia mutation L858F in sodium channel Nav1.7. *Mol. Pain.* 3:3. http://dx.doi.org/10.1186/1744-8069-3-3

Kang, J.Q., W. Shen, and R.L. Macdonald. 2006. Why does fever trigger febrile seizures? GABAA receptor γ2 subunit mutations associated with idiopathic generalized epilepsies have temperature-dependent trafficking deficiencies. *J. Neurosci.* 26:2590–2597. http://dx.doi.org/10.1523/JNEUROSCI.4243-05.2006

Lossin, C. 2009. A catalog of *SCN1A* variants. *Brain Dev.* 31:114–130. http://dx.doi.org/10.1016/j.braindev.2008.07.011

Lossin, C., D.W. Wang, T.H. Rhodes, C.G. Vanoye, and A.L. George Jr. 2002. Molecular basis of an inherited epilepsy. *Neuron.* 34:877–884. http://dx.doi.org/10.1016/S0896-6273(02)00714-6

Lossin, C., T.H. Rhodes, R.R. Desai, C.G. Vanoye, D. Wang, S. Carniciu, O. Devinsky, and A.L. George Jr. 2003. Epilepsy-associated dysfunction in the voltage-gated neuronal sodium channel *SCN1A*. *J. Neurosci.* 23:11289–11295.

Martin, M.S., K. Dutt, L.A. Papale, C.M. Dubé, S.B. Dutton, G. de Haan, A. Shankar, S. Tufik, M.H. Meisler, T.Z. Baram, et al. 2010. Altered function of the *SCN1A* voltage-gated sodium channel leads to gamma-aminobutyric acid-ergic (GABAergic) interneuron abnormalities. *J. Biol. Chem.* 285:9823–9834. http://dx.doi.org/10.1074/jbc.M109.078568

Mashimo, T., I. Ohmori, M. Ouchida, Y. Ohno, T. Tsurumi, T. Miki, M. Wakamori, S. Ishihara, T. Yoshida, A. Takizawa, et al. 2010. A missense mutation of the gene encoding voltage-dependent sodium channel (Nav1.1) confers susceptibility to febrile seizures in rats. *J. Neurosci.* 30:5744–5753. http://dx.doi.org/10.1523/JNEUROSCI.3360-09.2010

Oakley, J.C., F. Kalume, F.H. Yu, T. Scheuer, and W.A. Catterall. 2009. Temperature- and age-dependent seizures in a mouse model of severe myoclonic epilepsy in infancy. *Proc. Natl. Acad. Sci. USA.* 106:3994–3999. http://dx.doi.org/10.1073/pnas.0813330106

Ogiwara, I., H. Miyamoto, N. Morita, N. Atapour, E. Mazaki, I. Inoue, T. Takeuchi, S. Itohara, Y. Yanagawa, K. Obata, et al. 2007. Nav1.1 localizes to axons of parvalbumin-positive inhibitory interneurons: a circuit basis for epileptic seizures in mice carrying an *Scn1a* gene mutation. *J. Neurosci.* 27:5903–5914. http://dx.doi.org/10.1523/JNEUROSCI.5270-06.2007

Ohmori, I., K.M. Kahlig, T.H. Rhodes, D.W. Wang, and A.L. George Jr. 2006. Nonfunctional *SCN1A* is common in severe myoclonic epilepsy of infancy. *Epilepsia.* 47:1636–1642. http://dx.doi.org/10.1111/j.1528-1167.2006.00643.x

Rhodes, T.H., C. Lossin, C.G. Vanoye, D.W. Wang, and A.L. George Jr. 2004. Noninactivating voltage-gated sodium channels in

severe myoclonic epilepsy of infancy. *Proc. Natl. Acad. Sci. USA.* 101:11147–11152. http://dx.doi.org/10.1073/pnas.0402482101

Rhodes, T.H., C.G. Vanoye, I. Ohmori, I. Ogiwara, K. Yamakawa, and A.L. George Jr. 2005. Sodium channel dysfunction in intractable childhood epilepsy with generalized tonic-clonic seizures. *J. Physiol.* 569:433–445. http://dx.doi.org/10.1113/jphysiol.2005.094326

Rusconi, R., P. Scalmani, R.R. Cassulini, G. Giunti, A. Gambardella, S. Franceschetti, G. Annesi, E. Wanke, and M. Mantegazza. 2007. Modulatory proteins can rescue a trafficking defective epileptogenic $Na_v1.1$ Na^+ channel mutant. *J. Neurosci.* 27:11037–11046. http://dx.doi.org/10.1523/JNEUROSCI.3515-07.2007

Rusconi, R., R. Combi, S. Cestèle, D. Grioni, S. Franceschetti, L. Dalprà, and M. Mantegazza. 2009. A rescuable folding defective Nav1.1 (*SCN1A*) sodium channel mutant causes GEFS+: common mechanism in Nav1.1 related epilepsies? *Hum. Mutat.* 30:E747–E760. http://dx.doi.org/10.1002/humu.21041

Samani, K., G. Wu, T. Ai, M. Shuraih, N.S. Mathuria, Z. Li, Y. Sohma, E. Purevjav, Y. Xi, J.A. Towbin, et al. 2009. A novel *SCN5A* mutation V1340I in Brugada syndrome augmenting arrhythmias during febrile illness. *Heart Rhythm.* 6:1318–1326. http://dx.doi.org/10.1016/j.hrthm.2009.05.016

Spampanato, J., A. Escayg, M.H. Meisler, and A.L. Goldin. 2001. Functional effects of two voltage-gated sodium channel mutations that cause generalized epilepsy with febrile seizures plus type 2. *J. Neurosci.* 21:7481–7490.

Spampanato, J., A. Escayg, M.H. Meisler, and A.L. Goldin. 2003. Generalized epilepsy with febrile seizures plus type 2 mutation W1204R alters voltage-dependent gating of $Na_v1.1$ sodium channels. *Neuroscience.* 116:37–48. http://dx.doi.org/10.1016/S0306-4522(02)00698-X

Spampanato, J., J.A. Kearney, G. de Haan, D.P. McEwen, A. Escayg, I. Aradi, B.T. MacDonald, S.I. Levin, I. Soltesz, P. Benna, et al. 2004. A novel epilepsy mutation in the sodium channel *SCN1A* identifies a cytoplasmic domain for beta subunit interaction. *J. Neurosci.* 24:10022–10034. http://dx.doi.org/10.1523/JNEUROSCI.2034-04.2004

Tang, B., K. Dutt, L. Papale, R. Rusconi, A. Shankar, J. Hunter, S. Tufik, F.H. Yu, W.A. Catterall, M. Mantegazza, et al. 2009. A BAC transgenic mouse model reveals neuron subtype-specific effects of a generalized epilepsy with febrile seizures plus (GEFS+) mutation. *Neurobiol. Dis.* 35:91–102. http://dx.doi.org/10.1016/j.nbd.2009.04.007

Volkers, L., K.M. Kahlig, N.E. Verbeek, J.H.G. Das, M.J.A. van Kempen, H. Stroink, P. Augustijn, O. van Nieuwenhuizen, D. Lindhout, A.L. George Jr., et al. 2011. $Na_v1.1$ dysfunction in genetic epilepsy with febrile seizures-plus or Dravet syndrome. *Eur. J. Neurosci.* 34:1268–1275. http://dx.doi.org/10.1111/j.1460-9568.2011.07826.x

Webb, J., and S.C. Cannon. 2008. Cold-induced defects of sodium channel gating in atypical periodic paralysis plus myotonia. *Neurology.* 70:755–761. http://dx.doi.org/10.1212/01.wnl.0000265397.70057.d8

Yu, F.H., M. Mantegazza, R.E. Westenbroek, C.A. Robbins, F. Kalume, K.A. Burton, W.J. Spain, G.S. McKnight, T. Scheuer, and W.A. Catterall. 2006. Reduced sodium current in GABAergic interneurons in a mouse model of severe myoclonic epilepsy in infancy. *Nat. Neurosci.* 9:1142–1149. http://dx.doi.org/10.1038/nn1754

Yu, M.J., Y.W. Shi, M.M. Gao, W.Y. Deng, X.R. Liu, L. Chen, Y.S. Long, Y.H. Yi, and W.P. Liao. 2010. Milder phenotype with SCN1A truncation mutation other than SMEI. *Seizure.* 19:443–445. http://dx.doi.org/10.1016/j.seizure.2010.06.010